Central European Journal of Energetic Materials
ISSN 1733-7178; e-ISSN 2353-1843
Copyright © 2023 Łukasiewicz Research Network – Institute of Industrial Organic Chemistry, Poland

Cent. Eur. J. Energ. Mater. 2023, *20*(1): 14-35; DOI 10.22211/cejem/162761
Article is available in PDF-format, in colour, at:
https://ipo.lukasiewicz.gov.pl/wydawnictwa/cejem-woluminy/vol-20-nr-1/


Article is available under the Creative Commons Attribution-Noncommercial-NoDerivs 3.0 license CC BY-NC-ND 3.0.

Research paper

Effect of Aluminum Content on the Combustion Performance of HTPB/AP/Al Propellants under High Combustion Pressure

Jin-chao Han, Song-qi Hu, Cheng-long Chu, Lin-lin Liu*)
Northwestern Polytechnical University, China
* *E-mail:* lll@nwpu.edu.cn

Abstract: Combustion mechanisms of propellants under high combustion pressure are extremely important for the development of high-pressure solid rocket motors. The combustion characteristics of three HTPB propellants prepared with an aluminum content of 1%, 10%, and 18% were evaluated in this study by analyzing the extinguished propellant surface, the combustion flame, and the temperature profile in the combustion pressure range of 12-30 MPa. The results showed that the burning surface temperature of the three propellants increased from 425 to 535 and to 643 °C as the aluminum content was increased from 1% to 18%, resulting in a faster thermal decomposition rate of the binder than the thermal decomposition rate of the AP particles. Consequently, the morphology of the extinguished propellant surface evolved from concave into convex, and the higher the aluminum content, the more obvious became the convex morphology. The combustion flame height of the three propellants showed a downward trend when the combustion pressure was increased from 12 to 18 MPa, enhancing the heat feedback to the burning surface. The burning surface temperature of the three samples increased by 75, 105 and 189 °C, respectively, with the increase in combustion pressure, resulting in a more distinct degree of concave and convex morphology of the extinguished propellant surface. In addition, this demonstrated that the local heat and mass transfer might play a dominant role under high pressures.

Keywords: aluminum, HTPB propellants, propellant surface, high pressure combustion

1 Introduction

Solid rocket motors (SRMs) are widely used as the power unit in the aerospace field because of their simple structure, high reliability, miniaturization, and long-term storage capacity. Composite propellants composed of ammonium perchlorate (AP), aluminum (Al), and hydroxyl-terminated polybutadiene (HTPB) binder have been extensively used in many SRMs, but they suffer from a problem of incomplete energy release. High operating pressures could not only enhance the expanding power capability of the combustion gases, but also increase the combustion efficiency of propellants, leading to an increase in the propellant energy level. However, the burning rate of propellants is drastically increased under a high combustion pressures, which may cause a failure [1]. Therefore, it is essential to study the combustion performance of propellants to reveal their combustion mechanisms under high combustion pressures.

Dillier *et al.* [2-4] designed a new very high combustion pressure strand burner for the determination of the burning rates of AP/HTPB-composite propellants up to combustion pressures of 68.9 MPa. The results showed that an exponent break occurred above 20 MPa, and the pressure exponent was greater than one. The characteristic pressure where the exponent break occurred decreased with a decrease in AP particle size; monomodal and trimodal propellants had lower characteristic pressures than bimodal propellants. A change in AP concentration slightly affected the characteristic pressure, while the addition of aluminum decreased the characteristic pressure from 35.85 to 29 MPa.

Stephens *et al.* [5] tested the burning rate of propellants containing a bimodal oxidizer in a strand burner at combustion pressures up to 34.5 MPa. A significant conclusion was that the pressure exponent of the propellants increased from 0.75 to 1.08 on varying the fraction of coarse and fine AP particles from 80/20 to 40/60. The burning rate of the propellants was significantly reduced using a larger AP size, and the pressure exponent of these samples decreased to 0.57.

Thomas *et al.* [6] measured the burning rate of AP/HTPB propellants containing various AP concentrations and unimodal AP distributions at combustion pressures of 0-15.5 MPa. The burning rate of the evaluated propellants increased with an increase in AP concentration and a decrease in AP particle size. Moreover, the AP particle size had a greater effect on the burning rate than the AP concentration.

Aluminum powders are added to propellants because it can increase the combustion heat and inhibit unstable combustion [7]. However, condensed combustion products, classified into agglomerates and smoke oxide particles,

Copyright © 2023 Łukasiewicz Research Network – Institute of Industrial Organic Chemistry, Poland

were formed when aluminized propellants underwent combustion, in turn affecting the combustion performance of the propellants [8].

Stephens et al. [5] studied the effect of bimodal aluminum particle size on the high-pressure combustion performance of propellants. The results indicated that the burning rate pressure index of a propellant could be increased by both decreasing the particle size of the aluminum and increasing the content of nano-aluminum from less than 0.6 to more than 0.9 in the range of 4-34.5 MPa.

Yao *et al.* [9] studied the combustion characteristics of HTPB composite propellants containing different coated aluminum nano-powders over the combustion pressure range of 10-15 MPa. The results showed that the burning rate of propellants containing nickel acetylacetonate was the highest at different combustion pressures. However, the burning rates of propellants containing oleic acid and perfluorotetradecanoic acid were almost the same at different combustion pressures, and all of them were higher than the propellants containing untreated aluminum nano-powders only, within the range of combustion pressures studied.

Guo *et al.* [10] introduced the effect of organic fluoride for HTPB propellants with an aluminum content from 16% to 24%. The results indicated that a large particle size and residual active aluminum in the condensed combustion products increased with the aluminum content, but significantly decreased when organic fluoride was added. The burning rate of propellants containing organic fluoride was slightly higher than those of propellants without organic fluoride, and the melting aluminum particles on the burning surface was less agglomerated, indicating more complete aluminum combustion.

Anand *et al.* [11] reported the effects of coarse and fine AP sizes for propellants in the 1-10 MPa combustion pressure range. The results showed that the larger the coarse AP size, the larger the aluminum agglomerate size, and the size of agglomerates decreased with an increase of fine AP. In addition, the size of the agglomerates increased with combustion pressure due to acceleration of the aggregation speed of aluminum particles.

Dokhan *et al.* [12] measured the burning rate of composite propellants with bimodal aluminum distributions containing various amounts of ultrafine aluminum. The results showed that ultrafine aluminum burned in the region near the propellant burning surface, resulting in an increase of burning rate of the propellant. An interesting phenomenon observed by Yuan *et al.* [13] was that an agglomerate droplet ruptured and ejected liquid aluminium onto the burning surface. This was clearly captured for the first time, and lead to a slight decrease in agglomerate diameter. Jin *et al.* [14] studied the distribution of aluminum particles on the burning surface during combustion of a propellant by using

Copyright © 2023 Łukasiewicz Research Network – Institute of Industrial Organic Chemistry, Poland

digital in-line holography (DIH). The results showed that the mean diameters and agglomeration fractions in the height range of 0-1 mm were larger than those in the overall combustion field, and a second merging process of aluminum particles occurred at and up to 1 mm above the burning surface. In addition, Galfetti *et al.* [15] studied the combustion performance of nano-aluminized propellants, and compared it with micro-aluminized propellants. The results indicated that the burning rate of nano-aluminized propellants was faster than that of micro-aluminized propellants, with a lower agglomeration phenomena being observed in the combustion products.

Babuk *et al.* [16] reported the condensed combustion products size of aluminized propellants increased with a decrease in burning rate. A decrease in the burning rate from 8 to 5 mm·s^{-1} led to about 20% increase in the agglomerate diameter [17]. In addition, Ao *et al.* [18, 19] measured the size distributions of aluminum agglomerates in the range of 5.5-9 MPa. The results showed a decrease in the size of aluminum agglomerates with the increase of combustion pressure.

Yavor *et al.* [20] reported the effects of porous aluminum particles in propellants, in reducing aluminum agglomeration in a combustion pressure range of 1-34 atm. The results showed that porous aluminum particles produced smaller agglomerates than regular aluminum due to the high specific area, leading to a shorter ignition time and hence formation of smaller agglomerates. In addition, nickel-coated aluminum particles produced smaller agglomerates than regular aluminum [21].

Aluminum/polytetrafluoroethylene (Al/PTFE) reactive materials have much higher energy than traditional materials [22]. Sippel *et al.* [23] showed that the use of tailored Al/PTFE composite particles reduced aluminum agglomeration in propellants. The results indicated that Al/PTFE inclusion modified particles (70/30 wt.%) resulted in a reduction in the average coarse fraction agglomerate size from either 75.8 or 125 μm, respectively, to 25.4 μm, compared to similarly sized spherical and flake aluminum.

Many efforts have been made to investigate the effect of propellant formulations on the burning rate and combustion of aluminum particles in propellants, but there are few reports corresponding to the combustion performance of propellants under high combustion pressures. In addition, a large amount of carbon smoke and aluminum oxide smoke during the combustion of propellants hinders the observation of the combustion flame and burning surface, leading to insufficient understanding of the high-pressure combustion mechanisms of propellants. Therefore, the combustion performance of HTPB/AP/Al propellants with different aluminum contents was explored and analyzed from the quenched propellant surface, flame structure and combustion wave under

Copyright © 2023 Łukasiewicz Research Network – Institute of Industrial Organic Chemistry, Poland

high combustion pressures in this study. These results could provide valuable information for revealing the heat and mass transfer mechanisms of the gas-solid phase under high pressures and for regulating the combustion performance of HTPB/AP propellants.

2 Experimental

2.1 Raw materials of propellants

HTPB and AP with particles sizes of 104-150 and 178-250 μm, respectively, were purchased from Liming Research & Design Institute of Chemical Industry Co., Ltd. Aluminum powder with an average particle size of 10 μm was supplied by Shanghai ST-nano Science & Technology Co., Ltd. Di-octyl sebacate (DOS) and toluene di-isocyanate (TDI) were obtained from Yingkou Tianyuan Chemical Research Institute Co., Ltd.

2.2 Propellant formulas

Three types of HTPB/AP/Al propellants were designed in this study, which were cast under vacuum and cured with TDI at 50 °C during 5 days. The HTPB propellant formulas with different aluminum contents, denoted as H1, H2, and H3, are listed in Table 1.

Table 1. HTPB composite propellant formulas

Samples	Components [wt.%]				
	HTPB	AP	DOS	TDI	Al
H1	15	79	4	1	1
H2	9.375	78	2	0.625	10
H3	8.438	71	2	0.562	18

2.3 Apparatus and methods

The self-designed rapid depressurization extinction burner was composed of a combustion chamber, an end-cap, an aluminum diaphragm, an O-ring, and a Teflon sealing ring. The composition diagram of the burner is shown in Figure 1. The principle of rapid depressurization is that the aluminum diaphragm is broken by the high pressure gases generated during the combustion of the propellant, resulting in a fast depressurization in the chamber. The gases absorb a large amount of heat during the expansion, leading to a significant reduction of the heat feedback to the surface. Thus, the propellant cannot obtain the heat required to maintain the combustion and eventually extinguishes. The extinguished

Copyright © 2023 Łukasiewicz Research Network – Institute of Industrial Organic Chemistry, Poland

surface of the propellants was obtained under high combustion pressures through an appropriate selection of the thickness of the aluminum diaphragm.

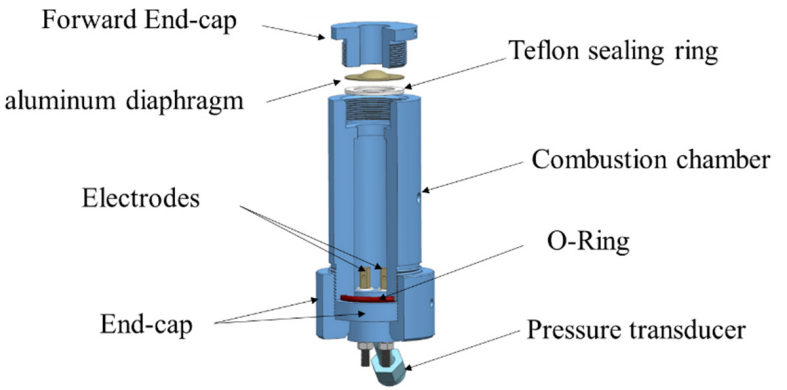

Figure 1. Rapid depressurization extinction burner

The morphology of the extinguished surface was analyzed using a DSX1000 optical digital microscope and TESCAN MIRA3 field-emission scanning electron microscope. The three-dimensional morphology of the quenched surface for the propellants was obtained with the optical microscope, and the combustion characteristics were analyzed according to the relative positions of each component in the propellant surface, while the scanning electron microscope could capture more detail of the combustion, such as AP particle surfaces and aluminum agglomerates. The combination of these two methods clarifies the combustion characteristics of the propellant more deeply. A high combustion pressure visualization experimental setup was used to obtain the temperature profile inside the propellant and combustion flame. The propellant strand, embedded with D-type (tungsten-3% rhenium and tungsten-25% rhenium) thermocouples in the middle of the propellant strand in order to obtain the temperature profile under steady-state combustion, was mounted on a mounting plate and ignited by a nichrome wire equipped with a 24 V, 5A DC power supply. A new thermocouple was required for each propellant strand and the thermocouple head could monitor all temperature changes without separate calibration. A schematic diagram of the embedded thermocouple is shown in Figure 2. A high-speed camera was used to capture images of the burning process at rates of up to 5,000 fps, with exposure times of 20 μs or less. Booster equipment was used to pressurize the burner to the pressure required for the experiment. A schematic of the experimental device for the combustion wave is shown in Figure 3.

Copyright © 2023 Łukasiewicz Research Network – Institute of Industrial Organic Chemistry, Poland

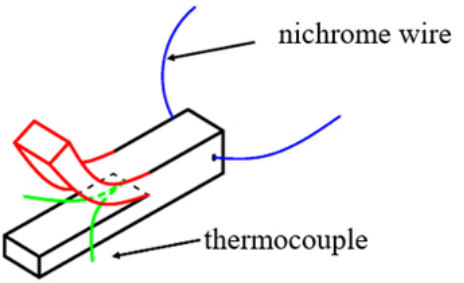

Figure 2. Schematic diagram of the embedded thermocouple

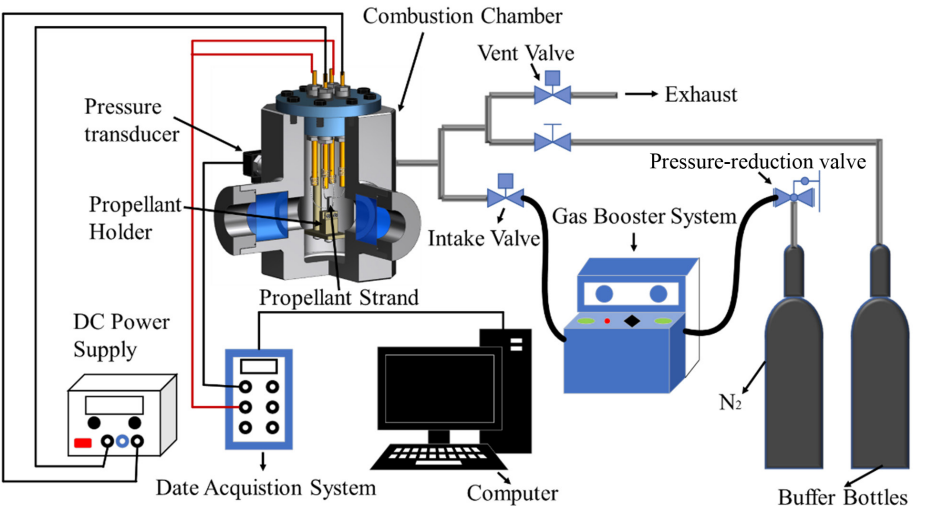

Figure 3. Schematic of the experimental device for combustion wave study

3 Results and Discussion

3.1 Characteristics of the extinguished propellant surface

The physical and chemical reaction information was obtained by analyzing the microscopic surface profiles and elemental distribution at the surface of the extinguished propellant samples, quenched by rapid depressurization, and subsequently the coupling mechanisms between the gas-phase and burning surface during the combustion under high pressure were revealed. Figure 4 presents the optical microscope images (at 250X) and height cloud map of the three propellants quenched at different combustion pressures.

Copyright © 2023 Łukasiewicz Research Network – Institute of Industrial Organic Chemistry, Poland

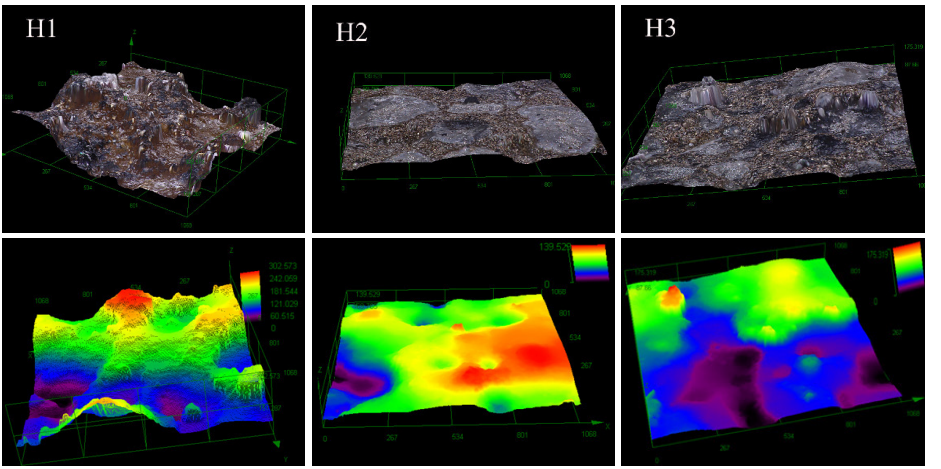

(a)

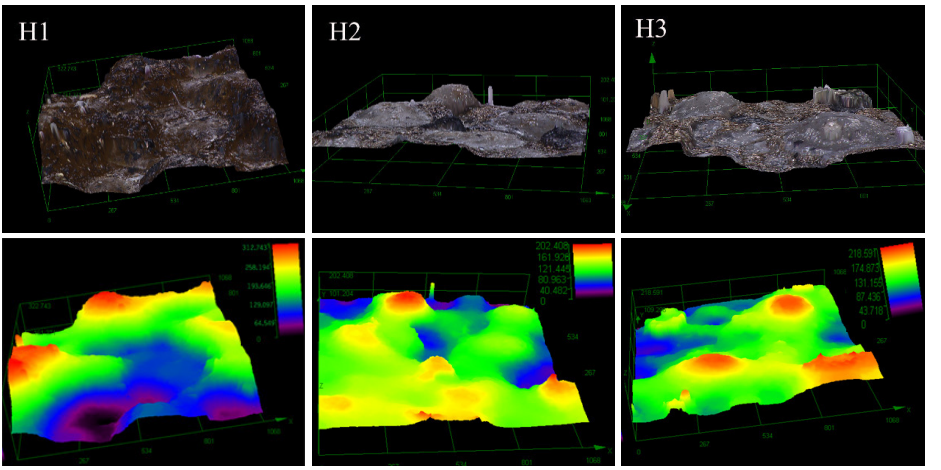

(b)

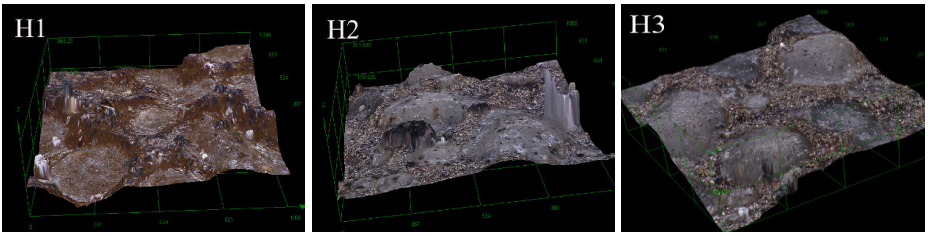

Copyright © 2023 Łukasiewicz Research Network – Institute of Industrial Organic Chemistry, Poland

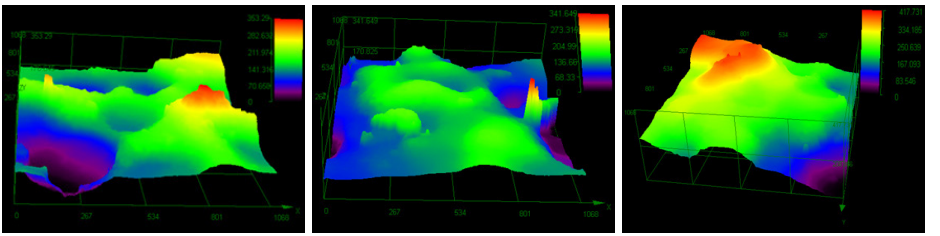

(c)

Figure 4. Images of the extinguished propellant surfaces obtained at different combustion pressures: 12 (a), 18 (b) and 30 MPa (c)

As shown in Figure 4(a), AP particles exposed on the surface of the H1 sample were concave, but slightly convex for samples H2 and H3 at 12 MPa. Meanwhile, it could be seen from the height cloud map of the propellant that the height variation of the burning surface for the H1 sample was around 302 μm, while for samples H2 and H3 were about 139 and 175 μm at 12 MPa, respectively. It is well known that the flame structure of AP/HTPB propellants is composed of the AP monopropellant flame, the primary diffusion flame, and the final diffusion flame. The AP monopropellant flame was located within a few microns above the surface and determined the combustion above the AP particles. The heat feedback region of the primary diffusion flame was smaller than that of the AP monopropellant flame, but the heat feedback from the primary diffusion flame to the burning surface was higher than that of the AP monopropellant flame owning to the high flame temperature. The final diffusion flame was formed when the AP monopropellant flame products and the primary diffusion flame products reacted above the burning surface. The position and shape of these three flames varied with the combustion pressure due to the difference in the chemical reaction rate and diffusion rate between AP and the binder.

The diffusion rate of the thermal decomposition products between AP and the binder was faster than the chemical reaction rate under low combustion pressures, and the thermal decomposition products reacted far away from the burning surface. Therefore, the heat feedback to the burning surface mainly came from the AP monopropellant decomposition flame and the primary diffusion flame, while the final primary flame was too far from the surface to reduce the heat feedback to the burning surface. Nevertheless, the chemical reaction rate was accelerated, and the diffusion reaction rate was inhibited under high combustion pressures. The thermal decomposition products between AP and the binder reacted at the near-burning surface. Thus, the final diffusion flame was also closer to the burning surface, resulting in a higher heat feedback to the

Copyright © 2023 Łukasiewicz Research Network – Institute of Industrial Organic Chemistry, Poland

burning surface. Meanwhile, the thermal decomposition rate of the binder was accelerated due to the increase in heat flux from the gas-phase, and the aluminum particles were more likely to be blown off the burning surface by the thermal decomposition airflow of binder and burned near the burning surface.

In addition, the thermal decomposition rate of AP particles was faster than that of the binder, which could be attributed to the differences in physical and chemical properties between AP and HTPB, and the thermal decomposition rate of AP and HTPB would increase with the increase in the heat feedback. The heat release and heat radiation by the combustion of aluminum particles had a low heat feedback to the burning surface due to the low aluminum content in the H1 sample. Thus, the difference in the thermal decomposition rates resulted in the concave shape of AP particles relative to the binder at 12 MPa. However, the heat release and heat radiation by the combustion of aluminum particles enhanced the heat feedback to the burning surface with the increase in aluminum content in sample H2, leading to a faster thermal decomposition rate of binder and oxidizer, and a larger number of aluminum particles were blown away from the burning surface by the thermal decomposition airflow. Thus, AP particles protruded above the burning surface. The degree of protrusion of AP particles in sample H3 was more obvious than that of sample H2 due to the increase in aluminum content.

Figure 4 shows that the protrusion and depression of the burning surface for the three samples became more distinct when the combustion pressure was increased from 12 to 30 MPa, and the height variation of the burning surface for sample H1 was increased from 302 to 353 μm. Similar results were observed for height variations for samples H2 and H3. The difference in the thermal decomposition rate between AP particles and the binder in sample H1 gradually increased with the combustion pressure; consequently, the concave degree of AP particles became more distinct. For sample H2, the protrusion of AP particles gradually became apparent with the increase in combustion pressure. The heat feedback of the combustion flame to the burning surface was enlarged due to the closer combustion flame under high combustion pressures, leading to a faster thermal decomposition rate of the binder, while a larger amount of aluminum agglomerates burned near the surface, resulting in more heat flux to the surface, and thus the protrusion degree of AP particles in the sample H2 increased with the increase in combustion pressure. In addition, it could also be seen from Figure 3 that the AP particles of sample H3 protruded significantly as the pressure was increased in comparison to sample H2, indicating that the heat flux from the combustion of aluminum agglomerates became more prominant with the increase in aluminum content under high combustion pressures. Furthermore, studying the results from the burning surface morphology with pressure also

Copyright © 2023 Łukasiewicz Research Network – Institute of Industrial Organic Chemistry, Poland

demonstrated that local heat and mass transfer might play a dominant role under high combustion pressures.

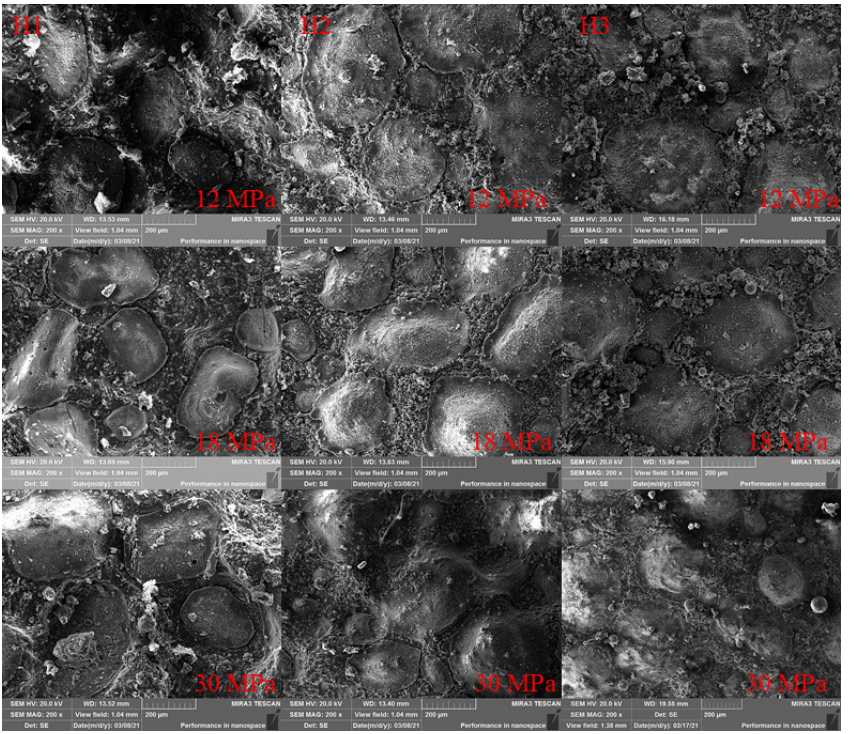

(a)

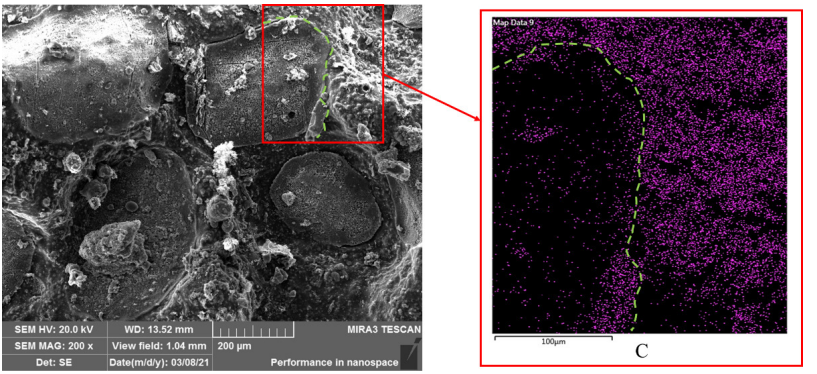

(b)

Figure 5. SEM images of the quenched surfaces and partial energy spectrum

Copyright © 2023 Łukasiewicz Research Network – Institute of Industrial Organic Chemistry, Poland

The increase in aluminum content increased the burning rate of the propellants, but agglomeration of the aluminum particles reduced the combustion efficiency of the aluminum. A high combustion pressure not only reduced the ignition temperature of aluminum particles, but also increased the burning rate of the propellants, resulting in reduced residence time of aluminum particles on the burning surface and smaller aluminum agglomerate size [24]. As shown in Figure 5(a), the size of aluminum agglomerates on the surface of the three propellants first decreased and then increased with the increase in aluminum content under 30 MPa. The residence time of aluminum particles on the burning surface was longer due to the lower thermal decomposition rate for sample H1 with low aluminum content, resulting in a larger size of the aluminum agglomerates [25]. The thermal decomposition rate of sample H2 was increased by the increase in aluminum content, and the residence time of aluminum particles on the burning surface decreased. Thus, the agglomerate size was smaller than for sample H1. However, the size of the aluminum agglomerates on the surface of sample H3 was larger than those of sample H2, which was caused by the high aluminum content and faster aggregation rate of aluminum particles under high combustion pressures. A similar trend was also observed by Anand [11], that the size of the agglomerates increased with an increase in combustion pressure.

Carbon exists in the binder matrix, and the flow of the binder melt layer could be obtained by the distribution of carbon on the extinguished propellant surface. It can be seen from Figure 5(b) that the AP particles of the three propellants were partially covered by the binder melt layer. AP particles exposed on the quenched surface were concave for sample H1 with low aluminum content, and the edges of the AP particles were covered by the binder melt layer, indicating that the primary diffusion flame extended to the side of the AP particles and enhanced the heat feedback to the AP particles. This resulted in a faster thermal decomposition rate of the AP particles under high combustion pressures. However, AP particles exposed on the quenched surface of samples H2 and H3 protruded above the surface, and the edge of the AP particles covered by the binder melt layer was flat. This can be attributed to the higher heat feedback from the combustion of aluminum particles at the near-burning surface. In addition, this phenomenon indicated that the primary diffusion flame might have moved slightly to the binder side of the particle/binder interface and almost covered the entire burning surface.

3.2 Propellant combustion flame characteristics

The profile of the burning surface is the result of the interaction between the combustion flame and the unburned propellant during the combustion, which could reflect the heat and mass transfer between the gas-phase and the burning

Copyright © 2023 Łukasiewicz Research Network – Institute of Industrial Organic Chemistry, Poland

surface. and The coupled combustion mechanisms between the gas-phase and the burning surface was revealed by analyzing the burning surface profile of the propellants under a high combustion pressure. The large amount of soot produced by propellant burning under high pressures could obscure the combustion flame, resulting in difficulty in observing the flame, therefore, the combustion process of the three propellants was recorded at 12 and 18 MPa, and the flame images of the three propellants under different combustion pressures are shown in Figures 6 and 7, respectively.

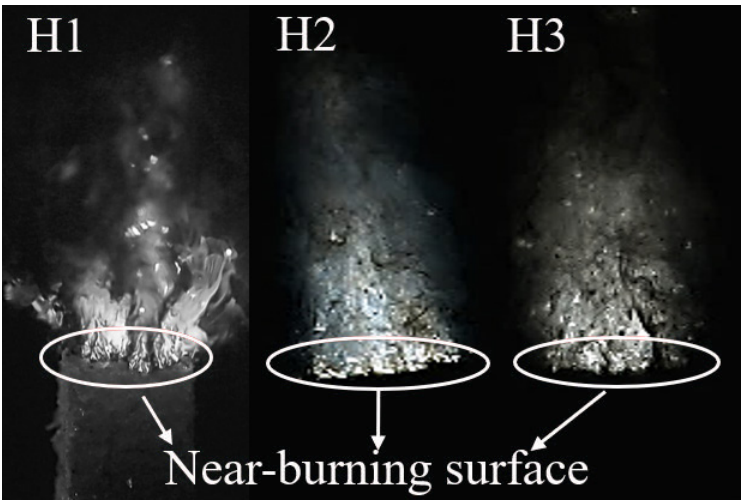

Figure 6. Combustion flame of propellant strands at 12 MPa

The thermal decomposition rate of AP and the binder was slow, and the diffusion rate was faster under a low combustion pressure, indicating that the reaction in the thermal decomposition products between AP and the binder was far away from the burning surface, leading to a higher flame height. However, the thermal decomposition rate of AP and the binder was accelerated, and the diffusion rate was suppressed, under high combustion pressures, resulting in the reaction of thermal decomposition products between AP and the binder at the near-burning surface. Thus, the flame height was reduced. In addition, aluminum is a metal fuel with low oxygen consumption and could release a large amount of heat during the combustion. This was transferred to the gas-phase and the burning surface through heat conduction and heat radiation, resulting in a faster gas-phase chemical reaction rate and thermal decomposition rate of the propellants. The oxygen consumption of aluminum during the combustion was lower than that of the binder, and the thermal decomposition products of the binder burned

Copyright © 2023 Łukasiewicz Research Network – Institute of Industrial Organic Chemistry, Poland

incompletely due to the lower oxygen-to-fuel ratio, resulting in a large amount of soot. However, the binder content with high oxygen consumption decreased with the increase in aluminum content, leading to a small amount of soot and a large amount of aluminum oxide smoke.

The 10 μm aluminum particles used in this study were more likely to be ignited by the primary diffusion flame during the diffusion and burn at the near-burning surface to form a dense aluminum burning region. Similar results were observed in the study by Dokhan *et al.* [26]. The heat released by the aluminum burning region not only increased the flame temperature of the propellants, resulting a faster gas-phase chemical reaction rate, but also enhanced the heat feedback to the burning surface, leading to faster thermal decomposition rates of AP and the binder. Figure 6 clearly shows that the AP particles burned faster than the surrounding binder for sample H1 with its low aluminum content, consistent with the results from the quenched surface shown in Figure 4(a) at 12 MPa. In addition, a large amount of smoke was observed during the combustion of sample H1 due to a lower oxygen-to-fuel ratio, indicating incomplete combustion of the thermal decomposition products of the binder. However, a small amount of soot and a large amount of aluminum oxide smoke were observed during the combustion processes of samples H2 and H3 because of the low binder content and high aluminum content. It can also be seen from Figure 6 that most of the aluminum particles burned at the near-burning surface, to form a dense aluminum burning region under 12 MPa, leading to the higher heat feedback to the burning surface. The burning surface of H2 and H3 propellants was relative flat, consistent with the morphology of the quenched surfaces shown in Figure 4(a) at 12 MPa.

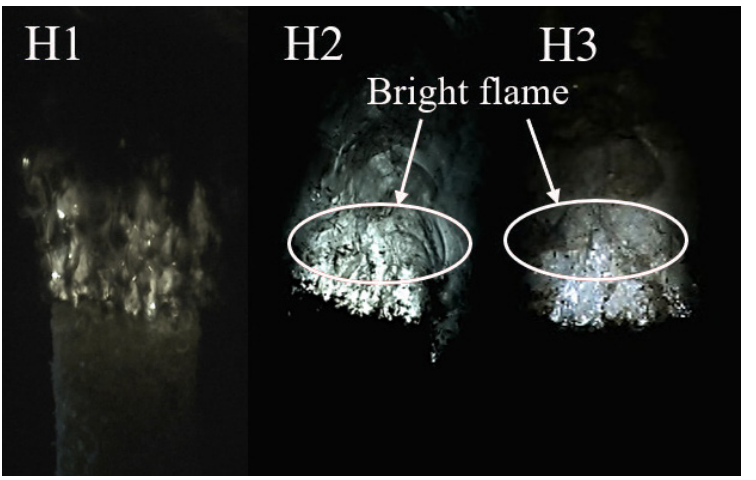

(a)

Copyright © 2023 Łukasiewicz Research Network – Institute of Industrial Organic Chemistry, Poland

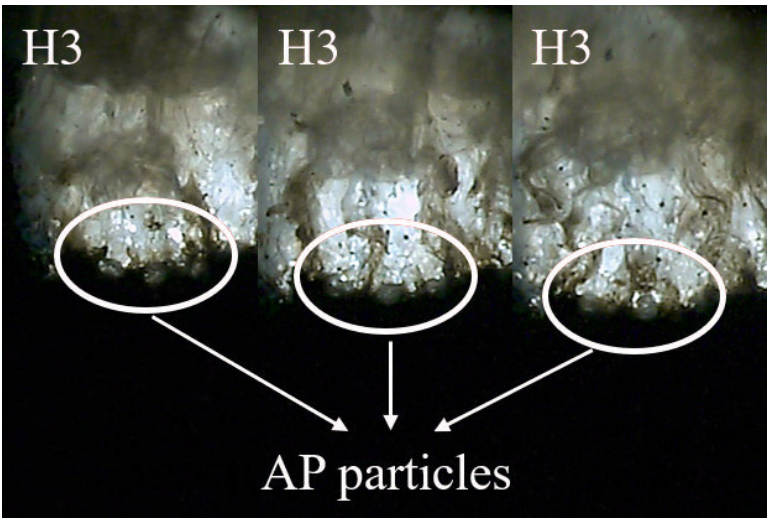

(b)

Figure 7. Combustion images of the propellant strands at 18 MPa: combustion images of H1, H2 and H3 samples (a), and partially enlarged images of sample H3 (b)

It can be seen from Figure 7(a) that a large amount of jet-like soot was generated during the combustion of propellant H1 due to the faster thermal decomposition rate of the binder at 18 MPa, which obscured the light of the flame, while the flame intensity of samples H2 and H3 was higher at 18 MPa compared with 12 MPa, indicating that the high combustion pressure helped to expose additional aluminum surface by the spreading and breakup of aluminum particles. In addition, the flame height from the three samples showed a downward trend and the unevenness of the burning surface became more obvious when the combustion pressure was increased from 12 to 18 MPa. These results are consistent with the conclusion obtained from the quenched surface in Figure 4(b) at 18 MPa. As shown in Figure 7(b), AP particles presented an obvious protrusion during the combustion, demonstrating that the binder burned faster than the AP particles, and also proved that the primary diffusion flame might move to the binder side of the particle/binder interface with an increase in aluminum content.

3.3 Temperature profile of propellants

The burning surface temperature and temperature gradient of the gas-phase and solid-phase regions could be determined from the temperature profile curves of the propellants, and subsequently heat transfer information between the

Copyright © 2023 Łukasiewicz Research Network – Institute of Industrial Organic Chemistry, Poland

gas-phase and the solid-phase was obtained. The temperature profiles from the three propellants at 12 and 18 MPa are shown in Figures 8 and 9, respectively, and temperature-time profiles were converted to temperature-distance profiles with burning rate data at different combustion pressures. The burning rates were measured using the target line test method, and the burning rates of the three propellants at 12 and 18 MPa are shown in Table 2. In addition, the slope of the temperature profile curve represented the temperature gradient of the condensed-phase and gas-phase regions. The thermal conductivity of the solid-phase was greater than that of the gas-phase, resulting in an abrupt change of the temperature gradient at the solid-gas interface. Consequently, an inflection point in the slope was observed in the temperature profile curve because of the difference in thermal conductivity of the two phases, which could be used to determine the burning surface position and temperature for the propellants.

Table 2. Burning rates of the three propellants at 12 and 18 MPa

Sample	Burning rate in [mm·s^{-1}]	
	12 MPa	18 MPa
H1	11.94	13.02
H2	12.44	14.67
H3	12.93	15.08

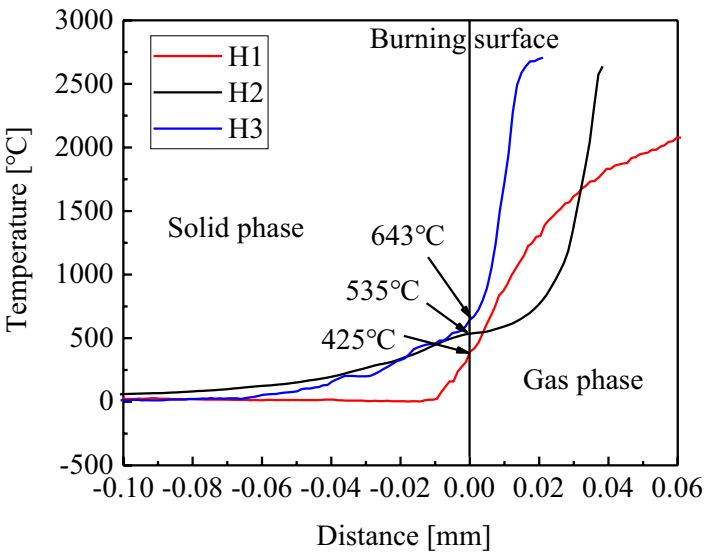

Figure 8. Temperature profiles of the propellants at 12 MPa

Copyright © 2023 Łukasiewicz Research Network – Institute of Industrial Organic Chemistry, Poland

The combustion flame was farther away from the burning surface and the heat flux to the surface was less under a low combustion pressure, resulting in a lower burning surface temperature. However, the heat flux to the burning surface was enhanced due to the closer flame standoff distance to the surface under a high combustion pressure, leading to an increase in the burning surface temperature. Furthermore, aluminum particles released a lot of heat during the combustion, which was transferred to the burning surface and the gas-phase region by convective heat transfer and radiation heat transfer. Thus, the combustion temperature, burning surface temperature, and temperature gradient of the two phases was increased. At the same time, aluminum absorbed the heat from the gas-phase region and transferred that heat to the solid-phase region due to the high thermal conductivity, resulting in an increase in the thickness of the solid-phase preheating region. As shown in Figure 8, the combustion temperature and burning surface temperature of sample H1 were low due to the low aluminum content at 12 MPa, resulting in a short solid-phase preheating zone and long gas-phase zone. However, the combustion temperature and burning surface temperature of samples H2 and H3, with the increased aluminum content, were greater than those of sample H1 at 12 MPa, which can be attributed to the large amount of heat released by combustion of the aluminum particles. Moreover, the solid-phase preheating zone of samples H2 and H3 was lengthened compared with that of sample H1 because the aluminum increased the thermal conductivity of the propellants. The increased thermal conductivity of aluminized propellants might facilitate their decomposition through the in-depth conductive heating of the solid-phase region.

Copyright © 2023 Łukasiewicz Research Network – Institute of Industrial Organic Chemistry, Poland

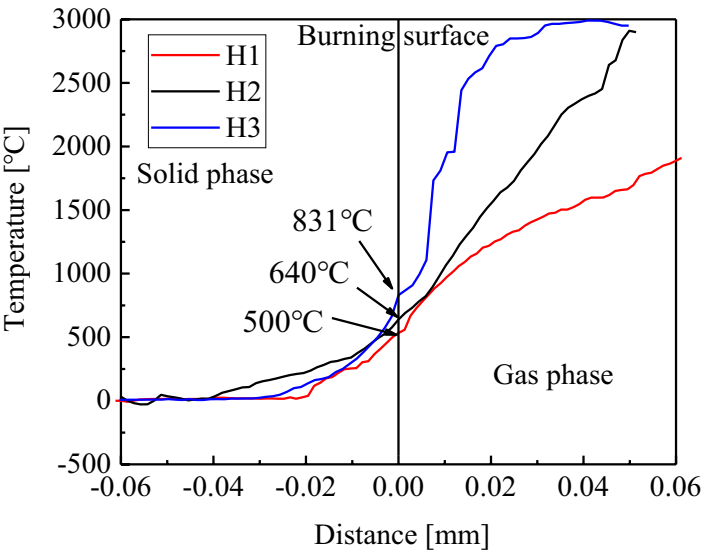

Figure 9. Temperature profiles of the propellants at 18 MPa

The combustion flame was closer to the burning surface at 18 MPa than at 12 MPa, resulting in a higher heat flux to the burning surface, and the heat radiated by the combustion of aluminum particles at the near-burning surface also further enhanced the heat feedback to the surface. In addition, aluminum particles and some HTPB binder within a pocket formed by coarse AP particles gradually melted to form aluminum agglomerates; the inside of these aluminum agglomerates might be heterogeneous and porous. The internal porous structure melted, decomposed, and reacted in the hot, sealed environment, emitting fuel-rich vapour [27]. The subsequent increase of combustion pressure inside the agglomerate led to the transient rupture and ejection phenomenon, which not only increased the combustion efficiency of the aluminum particles, but also enhanced the radiation heat transfer of aluminum particles to the burning surface. As shown in Figure 9, the combustion temperature and burning surface temperature of the three samples increased with the increase in aluminum content at 18 MPa, resulting in an increase in the temperature gradient. The thickness of the solid-phase preheating zone of the samples H2 and H3 was significantly greater than that of sample H1 due to the larger aluminum content, while the thickness of the gas-phase zone of samples H2 and H3 was shorter than that of sample H1. The burning surface temperature of the three samples increased by 75, 105 and 189 °C, respectively, when the combustion pressure was increased from 12 to 18 MPa. On the one hand, the standoff distance between the flame and the burning

Copyright © 2023 Łukasiewicz Research Network – Institute of Industrial Organic Chemistry, Poland

surface was closer because diffusion of the gaseous products was inhibited under high pressures, and the heat feedback to the burning surface was enhanced. On the other hand, the combustion of aluminum near the burning surface under high pressures also further enhanced the heat transfer to the surface. Therefore, the burning surface temperature increased with the increase in pressure. At the same time, this indicated that the heat transfer phenomenon of the flame to the burning surface was very obvious under high pressures, resulting in the increase in the propellant burning rate.

4 Conclusions

The combustion characteristics of three HTPB/AP/Al propellants were evaluated in this study by analyzing the extinguished propellant surface, the combustion flame and the temperature profile within the combustion pressure range of 12-30 MPa. The main conclusions are summarized below:

- The morphology of the extinguished propellant surface evolved from concave to convex with the increase in aluminum content from 1% to 18% at 12 MPa. The concave degree of the H1 propellant surface became more distinct with the increase in combustion pressure from 12 to 30 MPa, and the height variation of the burning surface for sample H1 was increased from 302 to 353 μm. The protrusion degree of AP particles gradually increased with the increase of combustion pressure for samples H2 and H3, and the height variations of the burning surface for samples H2 and H3 were both increased from about 100 μm to around 400 μm. In addition, the changes of the burning surface morphology with pressure indicated that local heat and mass transfer might be play a dominant role under high pressures.
- HTPB propellants with a high aluminum content would form a dense aluminum combustion zone located at the near-burning surface, which enhanced the heat feedback to the burning surface. The flame height exhibited a downward trend when the combustion pressure was increased from 12 to 18 MPa, indicating a closer flame standoff distance to the burning surface. The combustion efficiency of aluminum particles might increase with an increase in combustion pressure, resulting in an increase in the flame intensity.
- Aluminum not only released a lot of heat during the combustion, but also increased the thermal conductivity of the composite propellants. Thus, the burning surface temperature of the three propellants increased from 425 to 535 and to 643 °C with the increase in aluminum content under

Copyright © 2023 Łukasiewicz Research Network – Institute of Industrial Organic Chemistry, Poland

12 MPa. The combustion efficiency of aluminum particles also increased when the combustion pressure was increased from 12 to 18 MPa, resulting in a higher heat feedback to the burning surface. Therefore, the burning surface temperature of the three samples increased by 75, 105 and 189 ℃, respectively. This also indicated that the heat transfer phenomenon of flame to the burning surface was very obvious under high pressures, resulting in an increase in propellant burning rate.

Acknowledgement

This work is supported by the National Natural Science Foundation of China (Grant NO. 51776175).

References

[1] Atwood, A. I.; Ford, K.P.; Wheeler, C.J. High-Pressure Burning Rate Studies of Solid Rocket Propellants. *Prog. Propul. Phys.* **2013**, *4*: 3-14; DOI: 10.1051/eucass/201304003.

[2] Dillier, C.A.; Demko, A.; Stahl, J.; Reid, D.; Petersen, E.L. Temperature Sensitivity of AP/HTPB-based Rocket Propellants Using a New High-Combustion Pressure Strand Burner. *Proc. 55th* AIAA *Aerosp. Sci. Meet.,* Grapevine, TX, **2017**, 1-9.

[3] Dillier, C.A.; Petersen, E.D.; Sammet, T.; Rodriguez, F.A.; Thomas, J.C.; Petersen, E.L. Very-High-Combustion Pressure Burning Rates of AP/HTPB-composite Propellants with Varying AP Particle Sizes and Distributions. *Proc. Propulsion and Energy Forum*, Indianapolis, IN, **2019**, 1-6.

[4] Dillier, C.A.; Sammet, T.; Rodriguez, F.A.; Petersen, E.D.; Petersen, E.L. Aluminized and non-Aluminized AP/HTPB-composite Propellant Burning Rates at Very-High Combustion Pressures. *Proc. 27th Int. Colloq. on the Dynamics of Explosions and Reactive Systems (ICDERS)*, Beijing, China, **2019**, 1-6.

[5] Stephens, M.; Sammet, T.; Petersen, E.; Carro, R.; Wolf, S.; Smith, C. Performance of Ammonium-Perchlorate-Based Composite Propellant Containing Nanoscale Aluminum. *J. Propul. Power.* **2010**, *26*(3): 461-466; DOI: 10.2514/1.45148.

[6] Thomas, J.C.; Morrow, G.R.; Dillier, C.A.; Petersen, E.L. Comprehensive Study of AP Particle Size and Loading Effects on the Burning Rates of Composite AP/HTPB Propellants. *Proc. Propulsion and Energy Forum*, Cincinnati, OH, **2018**, 1-10.

[7] Liu, J.; Yuan, J.; Li, H.; Pang, A.; Xu, P.; Tang, G.; Xu, X. Thermal Oxidation and Heterogeneous Combustion of AlH_3 and Al: A Comparative Study. *Acta Astronaut*. **2021**, *179*: 636-645; DOI: 10.1016/j.actaastro.2020.11.039.

[8] Jeenu, R.; Pinumalla, K.; Deepak, D. Size Distribution of Particles in Combustion Products of Aluminized Composite Propellant. *J. Propul. Power*. **2010**, *26*(4):

Copyright © 2023 Łukasiewicz Research Network – Institute of Industrial Organic Chemistry, Poland

715-723; DOI: 10.2514/1.43482.
[9] Yao, E.; Zhao, F.; Xu, S.; Hu, R.; Xu, H.; Hao, H. Combustion Characteristics of Composite Solid Propellants Containing Different Coated Aluminum Nanopowders. *Adv. Mater. Res.* **2014**, *924*: 200-211; DOI: 10.4028/www.scientific.net/AMR.924.200.
[10] Guo, Y.; Li, J.; Gong, L.; Xiao, F.; Meng, L. Effect of Organic Fluoride on Combustion Performance of HTPB Propellants with Different Aluminum Content. *Combust. Sci. Technol.* **2021**, *193*(4): 1-14; DOI: 10.1080/00102202.2019.1669576.
[11] Anand, K.V.; Roy, A.; Mulla, I.; Balbudhe, K.; Jayaraman, K.; Chakravarthy, S.R. Experimental Data and Model Predictions of Aluminum Agglomeration in Ammonium Perchlorate-based Composite Propellants Including Plateau-burning Formulations. *Proc. Combust. Inst.* **2013**, *34*(2): 2139-2146; DOI: 10.1016/j.proci.2012.07.024.
[12] Dokhan, A.; Price, E.W.; Seitzman, J.M.; Sigman, R.K. The Effects of Bimodal Aluminum with Ultrafine Aluminum on the Burning Rates of Solid Propellants. *Proc. Combust. Inst.* **2002**, *29*(2): 2939-2945; DOI: 10.1016/S1540-7489(02)80359-5.
[13] Yuan, J.; Liu, J.; Zhou, Y.; Wang, J.; Xv, T. Aluminum Agglomeration of AP/HTPB Composite Propellant. *Acta Astronaut.* **2019**, *156*: 14-22; DOI: 10.1016/j.actaastro.2018.11.009.
[14] Jin, B.; Wang, Z.; Xu, G.; Ao, W.; Liu, P. Three-Dimensional Spatial Distributions of Agglomerated Particles on and near the Burning Surface of Aluminized Solid Propellant Using Morphological Digital In-Line Holography. *Aerosp. Sci. Technol.* **2020**, *106*(1) paper 106066: 1-14; DOI: 10.1016/j.ast.2020.106066.
[15] Galfetti, L.; DeLuca, L.T.; Severini, F.; Colombo, G.; Meda, L.; Marra, G. Pre and post-Burning Analysis of nano-Aluminized Solid Rocket Propellants. *Aerosp. Sci. Technol.* **2017**, *11*(1): 26-32; DOI: 10.1016/j.ast.2006.08.005.
[16] Babuk, V.A.; Dolotkazin, I.N.; Glebov, A.A. Burning Mechanism of Aluminized Solid Rocket Propellants Based on Energetic Binders. *Propellants Explos. Pyrotech.* **2005**, *30*(4): 281-290; DOI: 10.1002/prep.200500012.
[17] Liu, X.; Ao, W.; Liu, H.; Liu, P. Aluminum Agglomeration on Burning Surface of NEPE Propellants at 3-5 MPa. *Propellants Explos. Pyrotech.* **2017**, *42*(3): 260-268; DOI: 10.1002/prep.201600131.
[18] Ao, W.; Liu, P.; Yang, W. Agglomerates, Smoke Oxide Particles, and Carbon Inclusions in Condensed Combustion Products of an Aluminized GAP-based Propellant. *Acta Astronaut.* **2016**, *129*: 147-153; DOI: 10.1016/j.actaastro.2016.09.011.
[19] Liu, H.; Ao, W.; Liu, P.; Hu, S.; Lv, X.; Gou, D.; Wang, H. Experimental Investigation on the Condensed Combustion Products of Aluminized GAP-based Propellants. *Aerosp. Sci. Technol.* **2020**, *97* paper 105595: 1-11;DOI: 10.1016/j.ast.2019.105595.
[20] Yavor, Y.; Rosenband, V.; Gany, A. Reduced Agglomeration in Solid Propellants Containing Porous Aluminum. *J. Aerosp. Eng.* **2014**, *228*(10): 1857-1862; DOI: 10.1177/09544100134956.

Copyright © 2023 Łukasiewicz Research Network – Institute of Industrial Organic Chemistry, Poland

[21] Yavor, Y.; Rosenband, V.; Gany, A. Reduced Agglomeration Resulting from Nickel Coating of Aluminum Particles in Solid Propellants. *Int. J. Energ. Mater. Chem. Propul.* **2010**, *9*(6): 477-492; DOI: 10.1615/IntJEnergeticMaterialsChemProp.2011001385.
[22] Tang, E.; Luo, H.; Han, Y.; Chen, C.; Chang, M.; Guo, K.; He, L. Experimental Study on Burning of Two Al/PTFE Samples. *Appl. Therm. Eng.* **2020**, *180*: 115857; DOI: 10.1016/j.applthermaleng.2020.115857.
[23] Sippel, T.R.; Son, S.F.; Groven, L.J. Aluminum Agglomeration Reduction in a Composite Propellant Using Tailored Al /PTFE Particles. *Combust. Flame* **2014**, *161*: 311-321; DOI: 10.1016/j.combustflame.2013.08.009.
[24] Beckstead, M.W. A Summary of Aluminum Combustion. In: *Internal Aerodynamics in Solid Rocket Propulsion.* RTO EN-023 (AVT-096), **2004**, pp. 5/1-46; ISBN 92-837-1103-3.
[25] Ao, W.; Liu, X.; Rezaiguia, H.; Liu, H.; Wang, Z; Liu, P. Aluminum Agglomeration Involving the Second Mergence of Agglomerates on the Solid Propellants Burning Surface: Experiments and Modeling. *Acta Astronaut.* **2017**, *136*: 219-229; DOI: 10.1016/j.actaastro.2017.03.013.
[26] Dokhan, A.; Price, E.W.; Seitzman, J.M.; Sigman, R.K. The Ignition of Ultra-Fine Aluminum in Ammonium Perchlorate Solid Propellant Flames. *Proc. 39th* AIAA/ASME/SAE/ASEE Joint *Propul. Conf. and Exhibit*, Huntsville, AL, **2003**, 1-9; DOI: 10.2514/6.2003-4810.
[27] Geisler, R.L. A Global View of the Use of Aluminum Fuel in Solid Rocket Motors. *Proc. 38th* AIAA/ASME/SAE/ASEE Joint *Propul. Conf. and Exhibit*, Indianapolis, IN, **2002**, 1-8; DOI: 10.2514/6.2002-3748.

Received: December 23, 2021
Revised: March 28, 2023
First published online: March 31, 2023

Copyright © 2023 Łukasiewicz Research Network – Institute of Industrial Organic Chemistry, Poland